Formation Control of Nonholonomic Mobile Robots with Omnidirectional Visual Servoing and Motion Segmentation

René Vidal   Omid Shakernia   Shankar Sastry

Department of Electrical Engineering & Computer Sciences
University of California at Berkeley, Berkeley CA 94720-1772
{*rvidal,omids,sastry*}*@eecs.berkeley.edu*

Abstract— We consider the problem of having a team of nonholonomic mobile robots follow a desired leader-follower formation using omnidirectional vision. By specifying the desired formation in the image plane, we translate the control problem into a separate visual servoing task for each follower. We use a rank constraint on the omnidirectional optical flows across multiple frames to estimate the position and velocities of the leaders in the image plane of each follower. We show that the direct feedback-linearization of the leader-follower dynamics suffers from degenerate configurations due to the nonholonomic constraints of the robots and the nonlinearity of the omnidirectional projection model. We therefore design a nonlinear tracking controller that avoids such degenerate configurations, while preserving the formation input-to-state stability. Our control law naturally incorporates collision avoidance by exploiting the geometry of omnidirectional cameras. We present simulations and experiments evaluating our omnidirectional vision-based formation control scheme.

I. INTRODUCTION

The problem of controlling a formation of ground and aerial vehicles is gaining significant importance in the control and robotics communities thanks to applications in air traffic control, satellite clustering, automatic highways, and mobile robotics. Previous work in formation control (see Section I-B for a brief review) assumes that communication among the robots is available and concentrates on aspects of the problem such as stability, controller synthesis, and feasibility.

In the absence of communication, the formation control problem becomes quite challenging from a sensing viewpoint due to the need for simultaneous estimation of the motion of multiple moving objects. Das *et al.* [2] tackle vision-based formation control with feedback-linearization by employing a clever choice of coordinates in the configuration space. They mitigate sensing difficulties by painting each leader of a different color, and then using color tracking to detect and track the leaders.

A. Contributions of this paper

In this paper, we present a novel approach to vision-based formation control of nonholonomic robots equipped with central panoramic cameras in which the detection and tracking of the leaders is based solely on their motions on the image plane, as illustrated in Fig. 1.
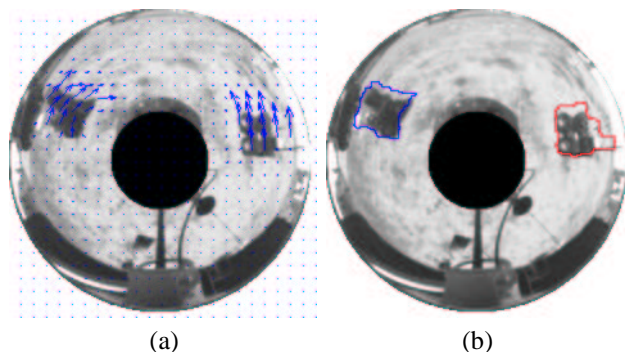

Fig. 1.   Motion segmentation for two mobile robots based on their omnidirectional optical flows.

Our approach is to translate the formation control problem from the configuration space into a separate visual servoing control task for each follower. In Section II we show how to estimate the position and velocities of each leader in the image plane of the follower by using a rank constraint on the central panoramic optical flow across multiple frames. We also derive the leader-follower dynamics in the image plane of the follower for a calibrated camera undergoing planar motion. In Section III we show that the direct feedback-linearization of the leader-follower dynamics suffers from degenerate configurations due to the nonholonomic constraints of the robots and the nonlinearity of the central panoramic projection model. We therefore design a nonlinear tracking controller that avoids such degenerate configurations, while maintaining the formation input-to-state stability. Our control law naturally incorporates collision avoidance by exploiting the geometry of central panoramic cameras. In Section IV we present simulations and experiments validating our omnidirectional vision-based formation control scheme. Section V concludes the paper.

B. Previous work

Swaroop *et al.* [10] proposed the notion of string stability for line formations and derived sufficient conditions for a formation to be string stable. Pant *et al.* [7] generalized string stability to formations in a planar mesh, through the concept of mesh stability. Tannner *et al.* [12]

concentrated on formations in acyclic graphs and studied the effect of feedback and feedforward on the input-to-state stability of the formation. Fax *et al.* [5] analyzed the stability of formations in arbitrary graphs and proposed a Nyquist-like stability criteria that can be derived from the spectral properties of the graph Laplacian. Egerstedt and Hu [4] propose the use of formation constraint functions to decouple the coordination and tracking problems, while maintaining the stability of the formation. Stipanovic *et al.* [9] studied the design of decentralized control laws that result in stable formations, provided that the leader's desired velocity is known. Desai *et al.* [3] proposed a graph-theoretic approach for coordinating transitions between two formations. Tabuada *et al.* [11] studied the conditions under which a desired formation is feasible, *i.e.* whether it is possible to design a trajectory that both maintains the formation and satisfies the kinematic constraints of the robots.

II. CENTRAL PANORAMIC FORMATION DYNAMICS

A. Central panoramic camera model and its optical flow

Central panoramic cameras are realizations of omnidirectional vision systems that combine a mirror and a lens and have a unique effective focal point. Building on the results of [6], we show in [8] that the image $(x, y)^T$ of a 3D point $q = (X, Y, Z)^T \in \mathbb{R}^3$ obtained by a calibrated central panoramic camera with parameter $\xi \in [0, 1]$ can be modeled as a projection onto the surface

$$z = \mathbf{f}_\xi(x, y) \triangleq \frac{-1 + \xi^2(x^2 + y^2)}{1 + \xi\sqrt{1 + (1 - \xi^2)(x^2 + y^2)}} \quad (1)$$

followed by orthographic projection onto the XY plane, as illustrated in Fig. 2. The composition of these two projections gives[1]:

$$\begin{bmatrix} x \\ y \end{bmatrix} = \frac{1}{-Z + \xi\sqrt{X^2 + Y^2 + Z^2}} \begin{bmatrix} X \\ Y \end{bmatrix} \triangleq \frac{1}{\lambda} \begin{bmatrix} X \\ Y \end{bmatrix}. \quad (2)$$

When the camera moves in the XY plane, its angular and linear velocities are given by $\Omega = (0, 0, \Omega_z)^T \in \mathbb{R}^3$ and $V = (V_x, V_y, 0)^T \in \mathbb{R}^3$, respectively. Relative to the camera, the point q evolves as $\dot{q} = \Omega \times q + V$. This induces a motion in the central panoramic image plane, which can be computed by differentiating (2) with respect to time. We show in [8] that the optical flow $(\dot{x}, \dot{y})^T$ induced by a central panoramic camera undergoing a planar motion (Ω, V) is given by:

$$\begin{bmatrix} \dot{x} \\ \dot{y} \end{bmatrix} = \begin{bmatrix} -y \\ x \end{bmatrix} \Omega_z + \frac{1}{\lambda} \begin{bmatrix} 1 - \rho x^2 & -\rho xy \\ -\rho xy & 1 - \rho y^2 \end{bmatrix} \begin{bmatrix} V_x \\ V_y \end{bmatrix}, \quad (3)$$

where $\lambda = -Z + \xi\sqrt{X^2 + Y^2 + Z^2}$ is an unknown scale factor, $z = \mathbf{f}_\xi(x, y)$ and $\rho \triangleq \xi^2/(1 + z)$.

[1]Notice that $\xi = 0$ corresponds to perspective projection, while $\xi = 1$ corresponds to paracatadioptric projection (parabolic mirror with orthographic lens).
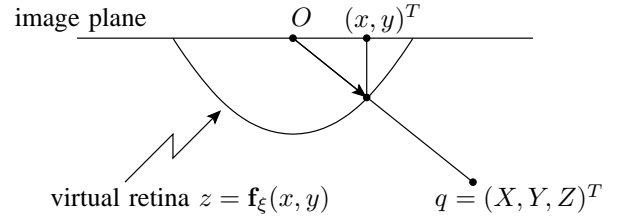

Fig. 2. Central panoramic projection model.

B. Central panoramic motion segmentation

Consider a central panoramic camera observing k leaders moving in the XY plane. We now describe how to estimate the image positions of the leaders from measurements of their optical flows across multiple frames. To this end, let $(x_i, y_i)^T$, $i = 1, \ldots, n$, be a pixel in the zeroth frame associated with one of the leaders and let $(\dot{x}_{ij}, \dot{y}_{ij})^T$ be its optical flow in frame $j = 1, \ldots, m$ relative to the zeroth. From (3) we have $\begin{bmatrix} \dot{x}_{ij} & \dot{y}_{ij} \end{bmatrix} = S_i M_j^T$ where

$$S_i = \begin{bmatrix} x_i & -y_i & \frac{1 - \rho_i x_i^2}{\lambda_i} & \frac{-\rho_i x_i y_i}{\lambda_i} & \frac{1 - \rho_i y_i^2}{\lambda_i} \end{bmatrix} \in \mathbb{R}^{1 \times 5}$$

$$M_j = \begin{bmatrix} 0 & \Omega_{zj} & V_{xj} & V_{yj} & 0 \\ \Omega_{zj} & 0 & 0 & V_{xj} & V_{yj} \end{bmatrix} \in \mathbb{R}^{2 \times 5}.$$

Therefore the *optical flow matrix* $W \in \mathbb{R}^{n \times 2m}$ associated with a single leader satisfies

$$W \triangleq \begin{bmatrix} \dot{x}_{11} & \dot{y}_{11} & \cdots & \cdots & \dot{x}_{1m} & \dot{y}_{1m} \\ \vdots & \vdots & & & \vdots & \vdots \\ \dot{x}_{n1} & \dot{y}_{n1} & \cdots & \cdots & \dot{x}_{nm} & \dot{y}_{nm} \end{bmatrix} = \tilde{S}\tilde{M}^T \quad (4)$$

where $\tilde{S} = [S_1^T \ S_2^T \cdots S_n^T]^T \in \mathbb{R}^{n \times 5}$ denotes the structure matrix and $\tilde{M} = [M_1^T \ M_2^T \cdots M_m^T]^T \in \mathbb{R}^{2m \times 5}$ denotes the motion matrix. We conclude that, for a single leader-follower configuration moving in the XY plane, the collection of central panoramic optical flows across multiple frames lies on a 5-dimensional subspace of $\mathbb{R}^{2m}$.

More generally, the optical flow matrix associated with k independently moving leaders can be decomposed as:

$$W = \begin{bmatrix} \tilde{S}_1 & \cdots & 0 \\ \vdots & \ddots & \vdots \\ 0 & \cdots & \tilde{S}_k \end{bmatrix} \begin{bmatrix} \tilde{M}_1^T \\ \vdots \\ \tilde{M}_k^T \end{bmatrix} = SM^T \quad (5)$$

where $S \in \mathbb{R}^{n \times 5k}$ and $M \in \mathbb{R}^{2m \times 5k}$. In practice, however, the optical flow matrix will not be block diagonal, because the segmentation of the image measurements is not known, *i.e.* we do not know which pixels correspond to which leader. We showed in [8] that one can recover the block diagonal structure of W, hence the segmentation of the image measurements, by looking at its leading singular vector $\mathbf{v}$. Since the entries of $\mathbf{v}$ are equal for pixels corresponding to the same leader and different otherwise, one can determine which pixels correspond

to which leader by thresholding $\mathbf{v}$. We use the center of gravity of each group of pixels as the pixel position for that leader. Note that, in practice, there will be an extra group of pixels corresponding to static points in the ground plane, whose motion is simply the motion of the camera. For a formation control scenario with few leaders, we can always identify this group of pixels as the largest one in the image. Since this group does not correspond to a leader, we do not compute its center of gravity.

C. Central panoramic leader-follower dynamics

Consider now the following nonholonomic kinematic model for the dynamics of each leader ℓ and follower f

$$\dot{X}_i = v_i \cos\theta_i, \quad \dot{Y}_i = v_i \sin\theta_i, \quad \dot{\theta}_i = \omega_i, \quad i = \ell, f \quad (6)$$

where the state $(X_i, Y_i, \theta_i) \in SE(2)$, and the inputs v_i and ω_i are the linear and angular velocities, respectively. Let $T_i = (X_i, Y_i, 0)^T \in \mathbb{R}^3$. We showed in [13] that the relative angular and linear velocities of leader ℓ relative to follower f, $\Omega_{\ell f} \in \mathbb{R}^3$ and $V_{\ell f} \in \mathbb{R}^3$, are given by:

$$\Omega_{\ell f} = \begin{bmatrix} 0 \\ 0 \\ 1 \end{bmatrix} (\omega_\ell - \omega_f), \quad V_{\ell f} = -\begin{bmatrix} 1 \\ 0 \\ 0 \end{bmatrix} v_f + \begin{bmatrix} F_{\ell f} \\ 0 \end{bmatrix} \quad (7)$$

where $F_{\ell f} \triangleq F_{\ell f}(T_\ell, T_f, \theta_\ell, \theta_f, v_\ell, \omega_\ell) \in \mathbb{R}^2$ is given by:

$$\begin{bmatrix} \cos(\theta_\ell - \theta_f) \\ \sin(\theta_\ell - \theta_f) \end{bmatrix} v_\ell - \begin{bmatrix} \cos(\theta_f) & \sin(\theta_f) \\ -\sin(\theta_f) & \cos(\theta_f) \end{bmatrix} \begin{bmatrix} -(Y_\ell - Y_f) \\ X_\ell - X_f \end{bmatrix} \omega_\ell.$$

Consider now a central panoramic camera mounted onboard each follower. We assume that the mounting is such that the camera coordinate system coincides with that of the follower, *i.e.* the optical center is located at $(X, Y, Z) = 0$ in the follower frame and the optical axis equals the Z axis. Therefore, we can replace the above expressions for $\Omega_{\ell f}$ and $V_{\ell f}$ in (3) to obtain the optical flow of a pixel associated with leader ℓ in the image plane of follower f as:

$$\begin{bmatrix} \dot{x} \\ \dot{y} \end{bmatrix} = -\begin{bmatrix} \frac{1-\rho x^2}{\lambda} & -y \\ \frac{-\rho xy}{\lambda} & x \end{bmatrix} \begin{bmatrix} v_f \\ \omega_f \end{bmatrix} + \begin{bmatrix} \frac{1-\rho x^2}{\lambda} & \frac{-\rho xy}{\lambda} & -y \\ \frac{-\rho xy}{\lambda} & \frac{1-\rho y^2}{\lambda} & x \end{bmatrix} \begin{bmatrix} F_{\ell f} \\ \omega_\ell \end{bmatrix}.$$

Since $z = \mathbf{f}_\xi(x, y)$ and $\lambda = Z/z$, if we assume a ground plane constraint, *i.e.* if we assume that $Z = Z_{\text{ground}} < 0$ is known, then we can write the equations of motion of a pixel as the drift-free control system

$$\begin{bmatrix} \dot{x} \\ \dot{y} \end{bmatrix} = H(x, y)\mathbf{u}_f + \mathbf{d}_{\ell f} \quad (8)$$

where $\mathbf{u}_f = (v_f, \omega_f)^T \in \mathbb{R}^2$ is the control action for the follower and $\mathbf{d}_{\ell f} \in \mathbb{R}^2$ can be thought of as an external input that depends on the state and control action of the leader and the state of the follower.

III. OMNIDIRECTIONAL VISUAL SERVOING

In this section, we design a control law $\mathbf{u}_f$ for each follower to keep a desired distance r_d and angle α_d from each leader in the image plane. That is, we assume that we are given a desired pixel location (x_d, y_d) for each leader, where $(x_d, y_d) = (r_d \cos(\alpha_d), r_d \sin(\alpha_d))$.

A. Visual servoing by feedback-linearization

Let us first apply feedback-linearization to the control system (8) with output $(x, y)^T$. We observe that the system has a well defined vector relative degree of $(1, 1)$ for all pixels (x, y) such that $H(x, y)$ is of rank 2, *i.e.* whenever $x \neq 0$ and $x^2 + y^2 \neq 1/\xi^2$. In this case, the relative degree of the system is $1 + 1 = 2$ thus the zero dynamics of the system are trivially exponentially minimum phase. Therefore the control law

$$\mathbf{u}_f = -H(x, y)^{-1} \left(\mathbf{d}_{\ell f} + \begin{bmatrix} k_1(x - x_d) \\ k_2(y - y_d) \end{bmatrix} \right) \quad (9)$$

results in a locally exponentially stable system around (x_d, y_d) whenever $k_1 > 0$ and $k_2 > 0$.

Notice however that the control law (9) is undefined whenever $x = 0$ or $x^2 + y^2 = 1/\xi^2$. The first degenerate configuration $x = 0$ arises from the nonlinearity of the central panoramic projection model and the nonholonomic constraints of the robots. For instance, consider a (static) point in the ground for which $x = 0$. Then the y component of the flow $\dot{y}$ is zero. Such a flow can be generated by purely translating the follower, or by purely rotating the follower, or by an appropriate rotation-translation combination. In other words, given the optical flow of that pixel, we cannot tell whether the follower is rotating or translating. Notice also that, due to the nonholonomic constraints of the robots, if $x = 0$ and $y - y_d \neq 0$, then the robot cannot instantaneously compensate the error since it cannot translate along its Y axis. On the other hand, the second degenerate configuration $x^2 + y^2 = 1/\xi^2$ corresponds to the set of pixels on the outer circle of an omnidirectional image. These pixels are projections of 3D points at infinity, *i.e.* they correspond to the horizon $z = 0$. Therefore, the degenerate configuration $x^2 + y^2 = 1/\xi^2$ is not so critical from a control point of view, because it can be avoided by assuming a finite arena. We therefore assume that $x^2 + y^2 \leq r_{\max}^2 < 1/\xi^2$, from now on.

B. Visual servoing by nonlinear feedback

Although the control law (9) guarantees locally that $(x(t), y(t)) \to (x_d, y_d)$ asymptotically, this requires that $x(t) \neq 0$ for all t and $x_d \neq 0$. Therefore,
  a) one cannot specify a desired formation with $x_d = 0$
  b) even if $x_d \neq 0$, the controller will saturate when the leader crosses the follower's Y axis at $x = 0$.

Since the latter case is fairly common in most formation configurations, we now design a slightly different controller that avoids this degeneracy, while maintaining the

input-to-state stability of the formation. We first rewrite the leader-follower dynamics in polar coordinates (r, α) so as to exploit the geometry of the central panoramic camera. The dynamics become:

$$\begin{bmatrix} \dot{r} \\ \dot{\alpha} \end{bmatrix} = - \begin{bmatrix} \frac{(1-\rho r^2)\cos(\alpha)}{\lambda} & 0 \\ -\frac{\sin(\alpha)}{r\lambda} & 1 \end{bmatrix} \begin{bmatrix} v_f \\ \omega_f \end{bmatrix} + \widetilde{\mathbf{d}}_{\ell f}, \qquad (10)$$

where $\widetilde{\mathbf{d}}_{\ell f}$ is the external input in polar coordinates. Rather than exactly inverting the dynamics as in (9), we use the pseudo-feedback linearizing control law:

$$\mathbf{u}_f = \begin{bmatrix} \frac{\lambda\cos(\alpha)}{(1-\rho r^2)} & 0 \\ \frac{\sin(\alpha)\cos(\alpha)}{r(1-\rho r^2)} & 1 \end{bmatrix} \left(\begin{bmatrix} k_1(r - r_d) \\ k_2(\alpha - \alpha_d) \end{bmatrix} + \widetilde{\mathbf{d}}_{\ell f} \right). \qquad (11)$$

With this controller, the closed-loop dynamics on the tracking errors $e_r = r - r_d$ and $e_\alpha = \alpha - \alpha_d$ become:

$$\begin{bmatrix} \dot{e_r} \\ \dot{e_\alpha} \end{bmatrix} = - \begin{bmatrix} k_1 \cos^2(\alpha)\, e_r \\ k_2\, e_\alpha \end{bmatrix} + \begin{bmatrix} \sin^2(\alpha) & 0 \\ 0 & 0 \end{bmatrix} \widetilde{\mathbf{d}}_{\ell f}. \quad (12)$$

Therefore, $\alpha(t) \to \alpha_d$ asymptotically when $k_2 > 0$. On the other hand, after solving the first order differential equation for the error e_r we obtain:

$$e_r(t) = e_r(t_0) \exp\left(-k_1 \int_{\tau=t_0}^{t} \cos^2(\alpha(\tau)) d\tau \right) +$$

$$\int_{\tau=0}^{t} \sin^2(\alpha(\tau)) \mathbf{d}_r(\tau) \exp\left(-k_1 \int_{\sigma=\tau}^{t} \cos^2(\alpha(\sigma)) d\sigma \right) d\tau$$

where $\mathbf{d}_r$ is the r component of $\mathbf{d}_{\ell f}$. A straightforward calculation shows that $|\mathbf{d}_r(t)| \leq |v_\ell(t)|/Z + |\omega_\ell(t)|$. Thus, if $k_1 > 0$, $\alpha(t) \neq \pm\pi/2$ from some t on, and the leader velocities (v_ℓ, ω_ℓ) are uniformly bounded, then the formation is input-to-state stable (ISS)[2]. Now, since $\alpha(t) = \alpha_d + e_\alpha(t_0) \exp(-k_2(t - t_0))$, the formation is ISS except when $\alpha_d = \pm\pi/2$ and $e_\alpha(t_0) = 0$. Furthermore, if the leader velocities are constant, so is the steady-state tracking error. One may overcome this error by adding an integral term to the controller (11).

Remark 3.1: Notice that the controller (11) is discontinuous at $e_\alpha = \pm\pi$ due to the identification of $\mathbb{S}^1$ with $\mathbb{R}$, together with the fact that the seemingly continuous feedback term $k_2 e_\alpha$ does not respect the underlying topology of $\mathbb{S}^1$. One could use smooth feedback instead, *e.g.* $k_2 \sin(\alpha)$, at the cost of a spurious critical point at $\pm\pi$. Since the topology of the annulus dictates that such spurious critical points are inevitable for smooth vector fields, we prefer the discontinuous controller (11) at the benefit of greater performance.

C. Estimation of the feedforward term

In order to implement either controller (9) or controller (11), we need to feedforward the unknown external input $\mathbf{d}_{\ell f} \in \mathbb{R}^2$. Although this term is a function of the

---

state and control of the leader and the state of the follower, we do *not* need to measure any of these quantities. Instead, we only need to estimate the two-dimensional vector $\mathbf{d}_{\ell f}$, which can be easily done from the output of the motion segmentation algorithm developed in Section II-B. To this end, let (x_w, y_w) and $(\dot{x}_w, \dot{y}_w)$ be the position and optical flow of a pixel that corresponds to a static 3D point in the world such that $x_w \neq 0$. From (8)[3], the velocities of the follower causing that optical flow are given by[4]:

$$\mathbf{u}_f = H(x_w, y_w)^{-1} \begin{bmatrix} \dot{x}_w \\ \dot{y}_w \end{bmatrix}. \qquad (13)$$

Now let (x_ℓ, y_ℓ) and $(\dot{x}_\ell, \dot{y}_\ell)$ be the position and optical flow of a pixel that corresponds to a 3D point on leader ℓ. From (8), the external disturbance can be estimated as:

$$\mathbf{d}_{\ell f} = \begin{bmatrix} \dot{x}_\ell \\ \dot{y}_\ell \end{bmatrix} - H(x_\ell, y_\ell) H(x_w, y_w)^{-1} \begin{bmatrix} \dot{x}_w \\ \dot{y}_w \end{bmatrix}. \qquad (14)$$

D. Collision avoidance

Although the control law (9) guarantees local stability of the leader-follower formation, it does not guarantee that the follower will not run into the leader. For example, imagine that the follower is initially in front of the leader and that the desired formation is with the follower behind the leader. Since the closed-loop dynamics are linear in the error $(x - x_d, y - y_d)$, the follower will apply a negative linear speed, and will most likely run into the leader.

Thanks to the geometry of central panoramic cameras, collisions can be avoided by ensuring that the leader stays far enough away from the center of the image. Effectively, our choice of image coordinates (r, α) for the controller (11) reveals the *safe* configurations as a simple constraint on r, namely $r_{\min} \leq r \leq r_{\max}$. Furthermore, the control law (11) is the gradient of a potential function

$$V(r, \alpha) = \frac{k_1(r - r_d)^2 + k_2(\alpha - \alpha_d)^2}{2}, \qquad (15)$$

which points transversely away from the safety boundary, and has a unique minimum at (r_d, α_d) (assuming $r_d > r_{\min}$). Following Cowan *et al.* [1], one can modify $V(r, \alpha)$ to yield a proper navigation function whose associated controller guarantees collision avoidance.

IV. EXPERIMENTAL RESULTS

We tested our segmentation algorithm in a real sequence. Fig. 1(a) shows one out of 200 frames taken by a paracatadioptric camera ($\xi = 1$) observing two moving robots. Fig. 1(b) shows the results of applying the segmentation algorithm in Section II-B. The sequence is correctly segmented into two independent motions.

---

[2]See [12] for the definition of formation input-to-state stability.

[3]Notice that the second term in (8) is zero in this case, because the point in 3D space is static, *i.e.* $(v_l, \omega_l) = (0, 0)$.

[4]Notice that in the presence of noise one may improve the estimation of $\mathbf{u}_f$ in (13) by using more than one pixel and solving the equations in a least squares sense.
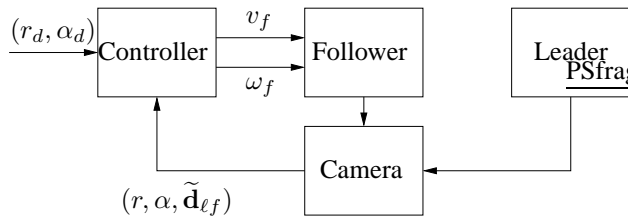
Fig. 3. Omnidirectional vision-based formation control scheme.

V-Formation   Line-Formation

Fig. 4. Formation configurations.

We tested our omnidirectional vision-based formation control scheme (see Fig. 3) by having three nonholonomic robots start in a V-Formation and then follow a Line-Formation with $(r_d, \alpha_d) = (1/\sqrt{2}, 0)$, as illustrated in Fig. 4. Since $\alpha_d = 0$, we choose to use controller (9) in *polar coordinates* with the parameters $\xi = 1$, $k_1 = 2.5$ and $k_2 = 1.76$. Fig. 5 shows the simulation results. For $t \in [0, 29]$ the leader moves with $v_\ell = 0.5$ and $\omega_\ell = 0$ and the followers move from the initial configuration to the desired one. Notice how the followers automatically avoid collision due to Follower1 trying to move in between Follower2 and the leader. For $t \in [29, 36]$ the leader changes its angular velocity to $w_\ell = 1$, thus moving in a circle. Follower1 starts rotating to the right to follow the leader, but soon realizes that the leader is coming towards it, and hence it backs up to avoid collision. For $t \in [36, 55]$ the leader changes its angular velocity to $w_\ell = 0$, and the followers are able to return to the desired formation. For $t \in [55, 60]$ the leader turns at $w_\ell = 0.5$ and the followers are able to keep the formation. For $t \in [60, 100]$ the leader turns at $w_\ell = 0.1$ and the followers maintain the formation into a line and a circle.

V. Conclusions and future work

We have presented a novel approach to formation control of nonholonomic mobile robots equipped with central panoramic cameras. Our approach uses motion segmentation techniques to estimate of the position and velocities of each leader, and omnidirectional visual servoing for tracking and collision avoidance. We showed that direct feedback-linearization of the leader-follower dynamics leads to asymptotic tracking, but suffers from degenerate configurations. We then presented a nonlinear controller that avoids singularities, but can only guarantee input-to-state stability of the formation.

Future work will include combining the two controllers presented in this paper in a hybrid theoretic formulation that allows the design of a feedback control law that avoids singularities and guarantees asymptotic tracking. We would also like to explore the design of alternative control laws that do not use optical flow estimates in the computation of the feedforward term. We also plan to implement our formation control scheme on the Berkeley test bed of unmanned ground and aerial vehicles.
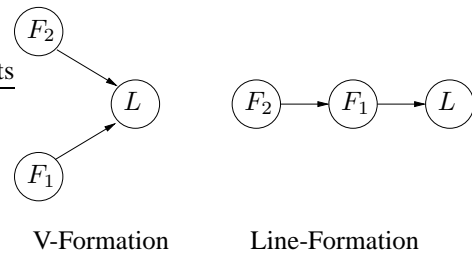
VII. REFERENCES

[1] N. Cowan, J. Weingarten, and D. Koditschek. Visual servoing via navigation functions. *IEEE Transactions on Robotics and Automation*, 18(4):521–533, 2002.

[2] A. Das, R. Fierro, V. Kumar, J. Ostrowski, J. Spletzer, and C. Taylor. A framework for vision based formation control. *IEEE Transactions on Robotics and Automation*, 18(5):813–825, 2002.

[3] J. Desai, J. Otrowski, and V. Kumar. Modeling and control of formations of nonholonomic robots. *IEEE Transactions on Robotics and Automation*, 17(6):905–908, 2001.

[4] M. Egerstedt and X. Hu. Formation constrained multi-agent control. *IEEE Transactions on Robotics and Automation*, 17(6):947–951, 2001.

[5] A. Fax and R. Murray. Graph laplacians and stabilization of vehicle formations. In *International Federation of Automatic Control World Congress*, 2002.

[6] C. Geyer and K. Daniilidis. A unifying theory for central panoramic systems and practical implications. In *European Conference on Computer Vision*, pages 445–461, 2000.

[7] A. Pant, P. Seiler, T. Koo, and K. Hedrick. Mesh stability of unmanned aerial vehicle clusters. In *American Control Conference*, pages 62–68, 2001.

[8] O. Shakernia, R. Vidal, and S. Sastry. Multibody motion estimation and segmentation from multiple central panoramic views. In *IEEE ICRA*, 2003.

[9] D. Stipanovic, G. Inalhan, R. Teo, and C. Tomlin. Decentralized overlapping control of a formation of unmanned aerial vehicles. In *IEEE Conference on Decision and Control*, pages 2829–2835, 2002.

[10] D. Swaroop and J. Hedrick. String stability of interconnected systems. *IEEE Transactions on Automatic Control*, 41:349–357, 1996.

[11] P. Tabuada, G. Pappas, and P. Lima. Feasible formations of multi-agent systems. In *American Control Conference*, pages 56–61, 2001.

[12] H. Tanner, V. Kumar, and G. Pappas. The effect of feedback and feedforward on formation ISS. In *IEEE ICRA*, pages 3448–3453, 2002.

[13] R. Vidal, O. Shakernia, and S. Sastry. Omnidirectional vision-based formation control. In *Fortieth Annual Allerton Conference on Communication, Control and Computing*, pages 1625–1634, 2002.
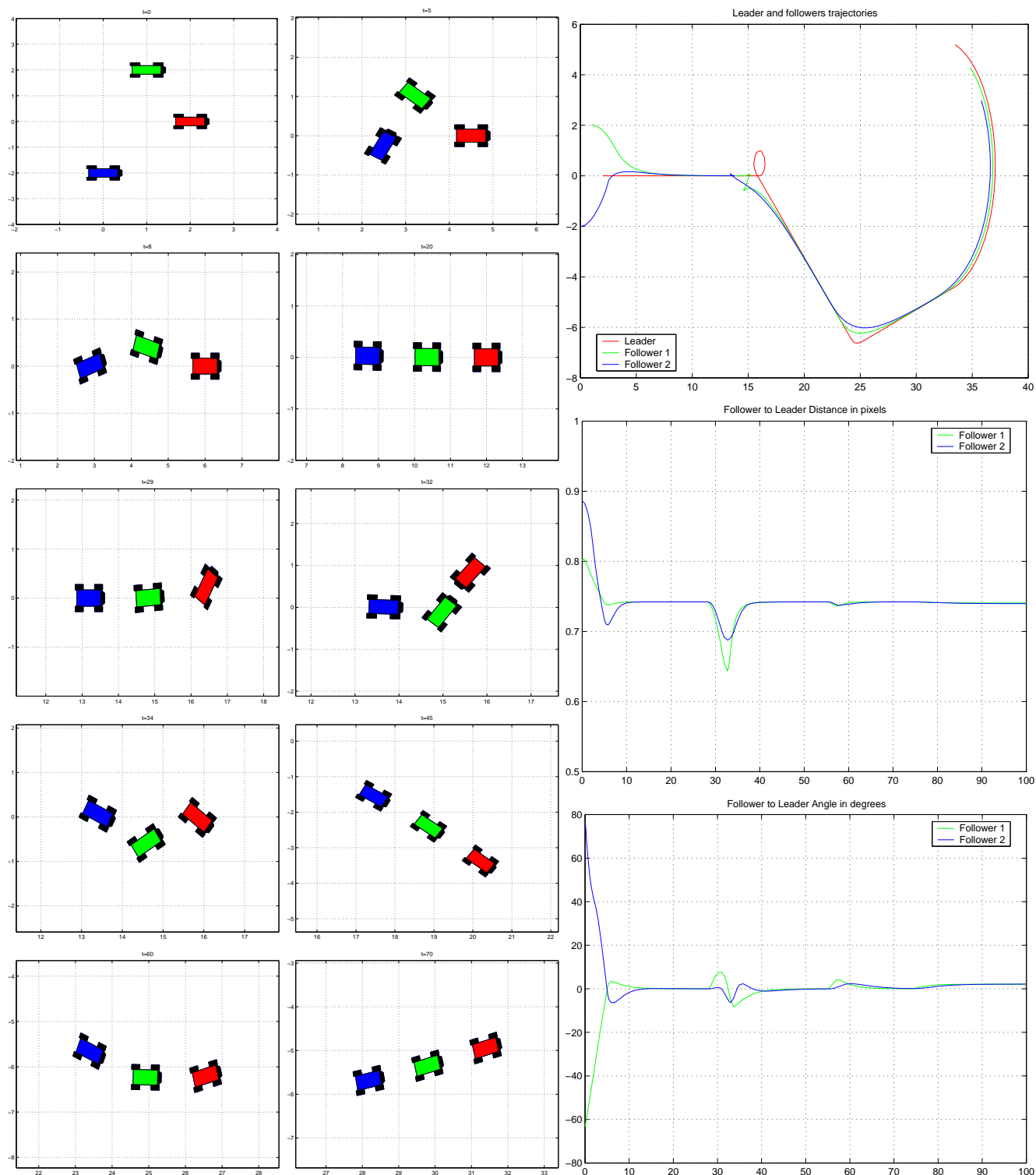
Fig. 5.   Simulation results for a Line-Formation. For $t \in [0, 10]$ the followers move from their initial V-Formation to the desired Line-Formation, while avoiding a collision due to Follower1 moving in between Follower2 and the leader. The leader abruptly rotates for $t \in [29, 36]$, but the followers are able to both avoid collision and later return to the desired line. For $t > 36$, they maintain their formation into a line, circle, line and a circle. Notice that it is not possible to maintain zero angular error during circular motion, because of the nonholonomic kinematic constraints of the robots.